Core Distortions and Geometries of the Difluorides and Dihydrides of Ca, Sr, and Ba

Ian Bytheway, Ronald J. Gillespie,* Ting-Hua Tang, and Richard F. W. Bader

Department of Chemistry, McMaster University, Hamilton, Ontario L8S 4M1, Canada

Received May 10, 1994[⊗]

Studies of the Laplacian of the calculated electron density ($\nabla^2\rho$) for the fluorides of Mg, Ca, Sr, and Ba, for the hydrides of Ca, Sr, and Ba, and for $Ca(CH_3)_2$ were undertaken in order to understand why these molecules with the exception of MgF_2 have a bent rather than a linear geometry. A linear geometry is expected on the basis of the simple ionic model or the VSEPR model and is observed for BeF_2 and MgF_2. The Laplacian distribution for the metal atom in each of the remaining molecules shows that the outer shell of its core is perturbed by the polarizing field of the ligands and is distorted in a manner corresponding to the presence of four approximately tetrahedrally localized concentrations of electronic charge. The angular shapes of these molecules can be understood in terms of the interaction between the distorted core and the ligands. In contrast, the distortion of the magnesium core in MgF_2 exhibits only two charge concentrations, one associated with each Mg−F bond, so that no deviation from the linear geometry is expected or found. This paper helps to establish the generality of the formation of localized concentrations of electronic charge in positions that are spatially opposed to the attached ligands, in the outer shell of the core of an element with accessible $(n - 1)$d orbitals, where n is the valence shell. The distortions of the cores of the heavier alkaline earth elements that are revealed by the Laplacian of the electron density have the same form as that proposed some years ago in an extension of the VSEPR model to account for the angular shape of these molecules.

Introduction

The structures of the alkaline earth dihalides in the gas phase have been of interest since it was discovered that some of these molecules are deflected in an electric field and therefore have a bent rather than linear geometry.[1] Subsequent studies by matrix isolation IR spectroscopy[2] and electron diffraction[3,4] have confirmed this initial observation. Although the bond angles are not known with great accuracy, it is well established that, among the alkaline earth dihalides, CaF_2, SrF_2, BaF_2, $CaCl_2$, $BaCl_2$, $SrBr_2$,[5] and BaI_2 are angular[4] with bond angles less than 150°, while the dihalides of beryllium and magnesium are linear.[3,4]

The bent geometry of CaF_2 and the other heavier group 2 dihalides is unexpected and is not explained by a simple ionic model or by the VSEPR model.[6] A basic assumption of the VSEPR model is that the core of the central atom in an AX_n molecule is spherical and has no influence on the arrangement of electron pairs in the valence shell and hence on the geometry of the molecule.[7,8] This is the case for most molecules of the main group elements, for which the VSEPR model is very successful. It was pointed out some time ago, however, that the core of some of the heavier main group elements and some transition metals may be sufficiently polarizable so that, in certain molecules, it is distorted to a nonspherical shape that may influence the geometry of the molecule.[7,8] In particular, it was proposed in an extension of the VSEPR model that, in the alkaline earth dihalides, interaction of the halide ligands with the metal core would cause some localization of the eight electrons of the outer shell of the core into four approximately tetrahedrally disposed pairs.[7,8] The negatively charged halogen ligands tend to avoid these partially localized electron pairs (electron pair domains) in the outer shell of the core by taking up positions opposite the faces of the tetrahedron of electron pair domains, thus giving an angular geometry.

It has been shown[9] that the Laplacian of the electron density reveals local concentrations of electronic charge in the valence shell of an atom in a molecule that have the same relative size, shape, and position as the electron pair domains postulated in the VSEPR model, thus providing a physical basis for this model. In this paper, we examine the Laplacian of the electron density of the fluorides and hydrides of Ca, Sr, and Ba and of calcium dimethyl in order to test and provide confirmation of the extended VSEPR model for these molecules.

Theoretical Methods

Calculations. There have been many ab initio studies[10−12] of the geometries of alkaline earth dihalides and related molecules at various levels of theory. These studies have demonstrated that large, flexible basis sets are needed to properly describe the geometries of these molecules. The basis sets employed in this study are detailed in Table 1, which gives the calculated energies and geometries obtained in MP2-(FULL) calculations using GAUSSIAN 92.[13] The basis set for strontium is that described by Kaupp et al.[11] in their study of the

[⊗] Abstract published in *Advance ACS Abstracts,* April 1, 1995.

(1) Wharton, L.; Berg, R. A.; Klemperer, W. *J. Chem. Phys.* **1963**, *39*, 2023.
(2) Calder, V.; Mann, D. E.; Sheshadri, K. S.; Allavena, M.; White, D. *J. Chem. Phys.* **1969**, *51*, 2093.
(3) Hargittai, M. In *Stereochemical Applications of Gas Phase Electron Diffraction*; Hargittai, I., Hargittai, M., Eds.; VCH: New York, 1988; Vol. B, p 383.
(4) Hargittai, M.; Hargittai, I. In *Structures and Conformations of Non-Rigid Molecules*; Laane, J., Dakkouri, M., van der Veken, B., Oberhammer, H., Eds.; NATO ASI Series C: Mathematical and Physical Sciences, Vol. 410; Kluwer: Dordrecht, The Netherlands, 1993.
(5) (a) Hargittai, M.; Kolonits, I.; Knausz, D.; Hargittai, I. *J. Chem. Phys.* **1992**, *96*, 8980. (b) Andersen, R. A.; Boncella, J. M.; Burns, C. J.; Blom, R.; Haaland, A.; Volden, H. V. *J. Organomet. Chem.* **1986**, *C49*, 312.
(6) Gillespie, R. J.; Nyholm, R. S. *Q. Rev. Chem. Soc.* **1957**, *11*, 339.
(7) Gillespie, R. J. *Molecular Geometry*; Van Nostrand Reinhold: London, 1972.
(8) Gillespie, R. J.; Hargittai, I. *The VSEPR Model of Molecular Geometry*; Allyn and Bacon and Prentice Hall International: Boston, MA, and London, respectively, 1991.
(9) Bader, R. F. W.; Gillespie, R. J.; MacDougall, P. J. *J. Am. Chem. Soc.* **1988**, *110*, 7329. Bader, R. F. W.; MacDougall, P. J.; Lau, C. D. H. *J. Am. Chem. Soc.* **1984**, *106*, 1594.

0020-1669/95/1334-2407$09.00/0

Table 1. Summary of the Results of the MP2(FULL) Calculations

molecule	basis set	energy (au)	R(M−L)[a]	∠L−M−L	ΔE_b* [b]
MgF_2	6-311G* [13]	−399.299 468	1.764	180.0	0.0
CaF_2	Ca(14s9p4d/8s4p4d)[c] F(6-31+G(2d))	−876.672 662	2.041 (2.048)	156.4	1.5
CaH_2	Ca(14s9p4d/8s4p4d)[c] H(6s2p)[d]	−678.178 455	2.030 (2.036)	157.0	0.5
$Ca(CH_3)_2$	Ca(14s9p4d/8s4p4d)[c] C,H(6-311++G(2d,2p))	−756.651 788	2.452 (2.458)	157.9	0.4
SrH_2	Sr(16s12p8d)[11] H(6s2p)[d]	−3130.409 521	2.174 (2.199)	136.9	1.3
SrF_2	Sr(16s12p8d)[11] F(6-31+G(2d))[13]	−3328.907 280	2.155 (2.184)	138.1	1.9
BaH_2	Ba(16s15p8d)[e] H(6s2p)[d]	−7879.467 802	2.281 (2.415)	116.4	7.5
BaF_2	Ba(16s15p8d)[e] F(6-31+G(2d))[13]	−8077.971 675	2.278 (2.344)	120.3	6.4

[a] Equilibrium bond length in Å. Parenthesized values are for optimized linear geometry. [b] Barrier to linear geometry in kcal mol^{-1}. [c] Wachters, A. J. H. *J. Chem. Phys.* **1970**, *52*, 1033. Added d functions from ref 10f. [d] Botschwina, P.; Meyer, W. *Chem. Phys.* **1977**, *20*, 43. [e] Huzinaga, S. *Gaussian Basis Sets for Molecular Calculations*; Elsevier: Amsterdam, 1984.

dihydrides of Ca, Sr, and Ba in which they also studied the use of 10-valence-electron pseudopotentials for the metal atoms. Huzinaga's basis set for Ba^{2+}, augmented with two diffuse p functions and four d functions as detailed by Kaupp et al.,[11] was used in the description of the barium-containing molecules because they are ionic in nature, the net charge on Ba in BaF_2 equaling +1.8 e.

The inclusion of the correlation of the core, as obtained in MP2-(FULL) calculations, give the results listed in Table 1. MP2 calculations with cores excluded from the correlation gave bond angles within 1° and bond lengths within ~0.04 Å of the values obtained by Kaupp et al.[11] for the hydrides of Ba and Sr using the 10-electron-valence pseudopotentials for the description of the cores. The same MP2 calculations gave bond angles and bond lengths smaller by 4° and 0.04 Å, respectively, than the results obtained for SrF_2 and BaF_2 by Seijo, Barandiaran, and Huzinaga,[10i] who also employed core model potentials. Their core potentials excluded the $(n-1)$p orbitals which were included in the valence set of the metal. These same authors conclude that relativistic effects are very small for the bond lengths and vibrational frequencies. The MP2(FULL) calculations yield only small further changes in the bond angles and bond lengths for the fluorides of approximately 1° and 0.003 Å, respectively, but for the hydrides of Sr and Ba the added correlation of the core causes the bond angles to decrease by another 5% and the bond lengths to decrease by another 0.08 Å compared to the values obtained using a 10-valence-electron pseudopotential. Thus a correlated core yields smaller bond angles than those obtained using model core potentials.

In agreement with previous calculations, the bond angle is found to decrease and the barrier to linearity to increase with increasing size of the metal atom. The bond angle is predicted to be characteristic of the metal atom, exhibiting only a small variation with ligand around the value of 157° for Ca, 138° for Sr, and 120.3° for Ba. The calcium dihydride and dimethyl molecules have barriers to attain linearity of less than 1 kcal mol^{-1} (Table 1). Kaupp and Schleyer,[12] in Hartree−Fock calculations coupled with a quasi-relativistic pseudopotential for the cores, found a negligible difference in energy between the linear and bent geometries for both CaF_2 and $Ca(CH_3)_2$ and described the molecules as quasilinear. They obtained barriers of 1.23 and 4.30 kcal mol^{-1} along with bond angles of 142 and 126° for SrF_2 and BaF_2, respectively.

Orbital Models. Schleyer and co-workers have summarized the electronic effects they believe responsible for the bent or linear geometries.[11,12,14,15] They ascribe bending to the polarization of the metal dication and to small but significant covalent σ-bonding contributions involving metal d orbitals, while the linear geometry is favored by anion−anion repulsion, by anion polarization, and by π-bonding between the appropriate ligand orbitals and acceptor π orbitals on the metal.

Polarized Ion Model. The structures of the group 2 dihalides have also been studied in terms of the polarized ion model. This model, originally proposed by Rittner[16] for the calculation of the force constants and dissociation energies of ionic diatomic molecules, has been applied to the alkaline earth dihalides by several authors, most recently by Guido and Gigli.[17] In this model, the energy is expressed in terms of the electrostatic contributions up to and including dipole−dipole interactions, an exponential repulsive energy, and a van der Waals attractive energy. It successfully predicts which dihalides are bent and which are linear and gives good agreement with experimental bond angles and dissociation energies. The model determines that the requirements for a bent geometry are a polarizable metal core and compact negatively charged ligands. The atomic populations and higher moments of the cores and ligands can be determined by the theory of atoms in molecules,[18] and in this manner, the geometry predictions obtained from the extended form of the VSEPR model can be compared with, and shown to complement, those obtained from the traditional polarized ion model.

Laplacian of the Electron Density and the VSEPR Model. The Laplacian of the electron density $\varrho(\mathbf{r})$ is defined as

$$\nabla^2\varrho = \partial^2\varrho/\partial x^2 + \partial^2\varrho/\partial y^2 + \partial^2\varrho/\partial z^2 \quad (1)$$

and is a scalar field which reveals the local structure of the electron density. The electron density is locally concentrated where $\nabla^2\varrho$ is negative and locally depleted where it is positive.[18] The purpose of the present work is to examine the nature and extent of the distortions of the cores of the calcium, strontium, and barium atoms in their difluorides and dihydrides, as determined by the localized charge concentrations exhibited by the Laplacian of the electron density and to relate the form of these distortions to the geometries of these

(10) (a) Hayes, E. F. *J. Phys. Chem.* **1966**, *70*, 3740. (b) Yarkonyi, D. R.; Hunt, W. J.; Schaeffer, H. F. *Mol. Phys.* **1973**, *26*, 941. (c) Gole, J. L.; Siu, A. K. Q.; Hayes, E. F. *J. Chem. Phys.* **1973**, *58*, 857. (d) Hassett, D. M.; Marsden, C. J. *J. Chem. Soc., Chem. Commun.* **1990**, 667. (e) Dyke, J. M.; Wright, T. G. *Chem. Phys. Lett.* **1990**, *169*, 138. (f) von Szentpaly, L.; Schwerdtfeger, P. *Chem. Phys. Lett.* **1990**, *70*, 555. (g) Salzner, U.; Schleyer, P. v. R. *Chem. Phys. Lett.* **1990**, *172*, 461. (h) DeKock, R. L.; Peterson, M. A.; Timmer, L. K.; Baerends, E. J.; Vernooijs, P. *Polyhedron* **1990**, *9*, 1919. (i) Seijo, L.; Barandiarán, Z.; Huzinaga, S. *J. Chem. Phys.* **1991**, *94*, 3762.
(11) Kaupp, M.; Schleyer, P. v. R.; Stoll, H.; Preuss, H. *J. Chem. Phys.* **1991**, *94*, 1360.
(12) Kaupp, M.; Schleyer, P. v. R. *J. Am. Chem. Soc.* **1992**, *114*, 491.
(13) Frisch, M. J.; Trucks, G. W.; Head-Gordon, M.; Gill, P. M. W.; Wong, M. W.; Foresman, J. B.; Johnson, B. G.; Schlegel, H. B.; Robb, M. A.; Replogle, E. S.; Gomperts, R.; Andres, J. L.; Raghavachari, K.; Binkley, J. S.; Gonzalez, C.; Martin, R. L.; Fox, D. J.; DeFrees, D. J.; Baker, J.; Stewart, J. J. P.; Pople, J. A. *Gaussian 92*; Gaussian, Inc.: Pittsburgh, PA, 1992.
(14) Kaupp, M.; Schleyer, P. v. R. *J. Am. Chem. Soc.* **1993**, *115*, 11202.
(15) Mösges, G.; Hampel, F.; Kaupp, M.; Schleyer, P. v. R. *J. Am. Chem. Soc.* **1992**, *114*, 10880.
(16) Rittner, E. S. *J. Chem. Phys.* **1951**, *19*, 1030.
(17) Guido, M.; Gigli, G. *J. Chem. Phys.* **1974**, *61*, 4138; **1976**, *65*, 1397.
(18) Bader, R. F. W. *Atoms in Molecules—A Quantum Theory*; Oxford University Press: Oxford, U.K., 1990.

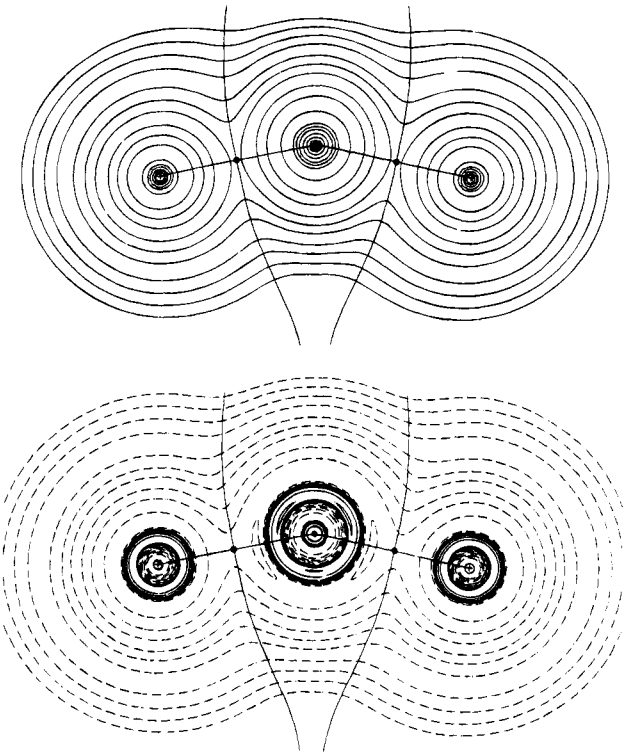

Figure 1. Contour maps of ϱ (top) and $\nabla^2\varrho$ (bottom) for the minimum-energy geometry of CaF_2, for which the F−Ca−F angle is 156.4°. The outer contour for ϱ is 0.001 au; the remaining contours change in steps of 2×10^n, 4×10^n, and 8×10^n au for n starting at −3 and increasing in steps of unity. In this and subsequent plots of $\nabla^2\varrho$, contours start at a zero value and change in steps of $\pm 2 \times 10^n$, $\pm 4 \times 10^n$, and $\pm 8 \times 10^n$ for n starting at −3 and increasing in steps of unity. Solid contours denote negative values of $\nabla^2\varrho$. The two LOCCC's in the outer core of the calcium atom can be seen in this plot of $\nabla^2\varrho$ as can the intersection of the broad extended maximum present in the plane perpendicular to this one. These are local maxima or (3,−3) critical points in $-\nabla^2\varrho$ (values in Table 3). The molecular graph and atomic boundaries are superimposed on these and subsequent plots, a solid circle denoting the position of a bond critical point.

molecules. The charge concentrations are local maxima or (3,−3) critical points in $-\nabla^2\varrho$, and this topological feature of the Laplacian of the electron density provides a measure of the tendency of the electrons to condense into spatially localized pairs.[9] Do the cores of these metal atoms exhibit a common pattern of electron localization and does it differ from that found in the core of magnesium in linear MgF_2? The description of the *distortions* present in a core as defined in terms of the topology of the Laplacian is distinct from the more usual description which relates the *polarization* of a core to its induced dipole and quadrupole moments.

An important property of the Laplacian of the electron density, not evident in the electron density itself, is that it recovers the shell structure of an atom.[18,19] The radii at which $-\nabla^2\varrho$ attains a maximum value define spheres upon which electronic charge is concentrated, there being one such sphere for each quantum shell. The radii of the spheres of charge concentration are characteristic for each shell of each atom and provide an unambiguous identification of the quantum shell in question.[20,21]

In covalent and polar covalent molecules, the presence of the ligands distorts the valence shell charge concentration, causing the formation of localized concentrations of electronic charge. The number and relative positions of these valence shell charge concentrations (VSCC's) have been shown to recover the number and relative positions of the localized electron pairs (electron pair domains) associated with the bonded and nonbonded electron pairs of the VSEPR model, thereby providing a physical basis for this model.[9,18] In the case of ionic molecules, for which one finds no valence shell concentration, the distortions revealed by the Laplacian can be used to examine the manner in which the electrons are spatially localized in the outer layer of the core.

Table 2. Metal−Ligand (L) Bond Critical Point Data and Atomic Charges in au

molecule	R(M−L) (Å)	ϱ_b	$\nabla^2\varrho_b$	r_b(M)	q(M)	q(L)
MgF_2	3.333	0.0730	0.7381	1.826	+1.760	−0.880
CaF_2	3.857	0.0730	0.4728	1.982	+1.778	−0.889
CaH_2	3.836	0.0466	0.1202	2.215	+1.670	−0.835
$Ca(CH_3)_2$	4.633	0.0452	0.1453	2.214	+1.652	−0.826
SrH_2	4.108	0.0445	0.0896	2.446	+1.656	−0.828
SrF_2	4.073	0.0695	0.4000	2.162	+1.806	−0.903
BaH_2	4.311	0.0481	0.0669	2.652	+1.594	−0.797
BaF_2	4.305	0.0671	0.3214	2.358	+1.798	−0.899

Analyses of the atomic properties and analyses of the electron density and its Laplacian were performed using the AIMPAC suite of programs.[22] A molecule is partitioned by surfaces of zero flux in the gradient vector field of $\varrho(\mathbf{r})$ into proper open systems, bounded regions of real space which are unique in that their properties are predicted by the action principle of quantum mechanics.[23] Such proper open systems have been identified with the atoms of chemistry.[24] The expectation values of the observables for the atoms complement the corresponding properties of the molecule of which they are a part.

Results and Discussion

Bent Molecules of Ca, Sr, and Ba. Contour plots of the electron density and its Laplacian for the equilibrium geometry of CaF_2 calculated at the MP2 level of theory are shown in Figure 1. Bond paths (lines of maximum electron density)[13] linking nuclei and zero-flux surfaces (surfaces which partition the molecule into its constituent atoms) are shown. Only two shells of charge concentration, in addition to the spike-like peak at the nucleus for the innermost shell, are present on the Ca showing that the fourth shell, the VSCC, is absent. The VSCC is absent from the metal atom in all of the molecules studied here and is consistent with the bonding to the metal being predominantly ionic. We have found previously[25] that when the magnitude of the charge on fluorine in an MF_n molecule is greater than 0.8, no valence shell charge concentration is found for M, although there is still some electron density in its valence shell. The atomic populations, obtained as the expectation values of the number operator over the atomic basins, are given in Table 2, and this charge transfer criterion is satisfied for all of the systems. Table 2 also lists the values of the density and its Laplacian at the bond critical point, ϱ_b and $\nabla^2\varrho_b$, together with its distance from the metal nucleus r_b(M). The small values of ϱ_b, the positive values of $\nabla^2\varrho_b$, and the ionic values for the radii all indicate ligand−metal interactions dominated by a transfer of density approaching the equivalent of two electronic charges with the density separately localized in each of the atomic basins to give closed-shell or ionic interactions. The values given in Table 2 can be contrasted with those for the C−H interaction in a methyl group of the dimethyl compound which are typical of a shared interaction: small charges with q(H) = −0.06, a large accumulation and concentration of electron density in the bond, $\varrho_b = 0.266$, $\nabla^2\varrho_b = -0.904$, and the bonded radius of carbon linked to H equals 1.292 au compared to the much larger value of 2.420 au in the Ca−C

(19) Bader, R. F. W.; Essén, H. *J. Chem. Phys.* **1984**, *80*, 1943.
(20) Sagar, R. P.; Ku, A. C. T.; Smith, V. *J. Chem. Phys.* **1988**, *88*, 4367.
(21) Shi, Z.; Boyd, R. J. *J. Chem. Phys.* **1988**, *88*, 4375.
(22) Biegler-König, F. W.; Bader, R. F. W.; Tang, T.-H. *J. Comput. Chem.* **1982**, *3*, 317.
(23) Bader, R. F. W. *Phys. Rev.* **1994**, *B49*, 13348.
(24) Bader, R. F. W.; Popelier, P. L. A.; Keith, T. A. *Angew. Chem., Int. Ed. Eng.* **1994**, *33*, 620.
(25) Bytheway, I.; Gillespie, R. J.; de Witte, R. S.; Bader, R. F. W. *Inorg. Chem.* **1994**, *33*, 2115.

Table 3. Critical Point Data for Charge Concentrations in the Outer Cores of Metal Atoms in au

molecule	type of (3,−3)	value of $\nabla^2\varrho$	r(M)	∠C−M−C (deg)	∠L−M−L (deg)
MgF_2	BCCC (2)	−57.913	0.389	180.0	180.0
CaF_2	LOCCC (2)	−4.185	0.899	124.2	156.4
	NBCCC (1)	−4.072	0.900		
CaF_2	LOCCC (2)	−4.274	0.899	118.2	140.0
	NBCCC (2)	−4.112	0.899	52.9	
SrF_2	LOCCC (2)	−0.239	1.299	110.0	138.1
	NBCCC (2)	−0.115	1.303	90.2	
BaF_2	LOCCC (2)	−0.101	1.670	107.0	120.3
	NBCCC (2)	−0.023	1.674	120.4	
$Ca(CH_3)_2$	LOCCC (2)	−4.171	0.898	128.6	157.9
	NBCCC (1)	−4.100	0.900		
$Ca(CH_3)_2$	LOCCC (2)	−4.357	0.900	112.4	109.5
	NBCCC (2)	−4.160	0.899	119.2	
CaH_2	LOCCC (2)	−4.166	0.898	125.6	157.0
	NBCCC (1)	−4.121	0.900		
CaH_2	LOCCC (2)	−4.367	0.900	111.7	109.5
	NBCCC (2)	−4.181	0.899	119.6	
SrH_2	LOCCC (2)	−0.242	1.298	109.1	136.9
	NBCCC (2)	−0.123	1.301	111.6	
BaH_2	LOCCC (2)	−0.124	1.689	104.2	116.4
	NBCCC (2)	−0.037	1.674	137.0	

interaction. Note the similarity in the properties of the Ca−H and Ca−C bonds, a result of their very similar electron-withdrawing abilities and the resulting ionic nature of the interactions. The ellipticity of the Ca−C bonds is quite small, equal to 0.008, whose orientation is indicative of a very small preferred accumulation of electron density in the plane of the H−C−Ca−C−H nuclei and hence of a nearly vanishing π-like interaction of the ligands with the metal atom. Thus, to a reasonable approximation, we can regard all of the molecules as being predominantly ionic, that is, as consisting of a M^{2+} ion and two negatively charged ligands.

The charge concentration corresponding to the outer shell of the core of the Ca atom shown in the Laplacian map, Figure 1, is not uniform but is distorted to form localized charge concentrations similar to those found in the valence shell of a covalent molecule. The properties of the charge concentrations are given in Table 3. The complete atomic graph[18] was determined for the shell in question to ensure that no CC's (3,−3) critical points in $-\nabla^2\varrho$, had been missed. There is a charge concentration (CC) in the outer shell of the core opposite each fluorine which we call a ligand-opposed core charge concentration (LOCCC). In addition, one sees the intersection of another charge concentration which is present in the plane perpendicular to the plane of the nuclei and is of broad extent. When the bond angle is reduced to the experimental value of 140°, the concentration of charge in the perpendicular plane is split in two giving two charge concentrations that we call nonbonding core charge concentrations (NBCCC's) because they are not associated with the ligands (Table 3). The arrangement of the CCC's becomes more truly tetrahedral as the F−Ca−F angle is reduced to 109.5°, Figure 2.

Calcium dihydride and dimethyl, like the difluoride, exhibit three CC's in the outer shell of the Ca core in their equilibrium geometries and a tetrahedral-like pattern of four core charge concentrations (CCC's) when further bent, Table 3. All of the remaining compounds possess smaller equilibrium bond angles and all exhibit four CCC's, two LOCCC's, and two NBCCC's, in the outer shell of the metal core in their equilibrium geometries. This is illustrated for SrF_2 and BaH_2 in Figure 3, diagrams which also indicate that the maxima occur in the fourth and fifth shells, respectively, of the two metal atoms. The distances of the maxima from the metal nucleus, 0.90 for Ca, 1.30 for Sr, and 1.68 au for Ba, are the characteristic radii[18,21]

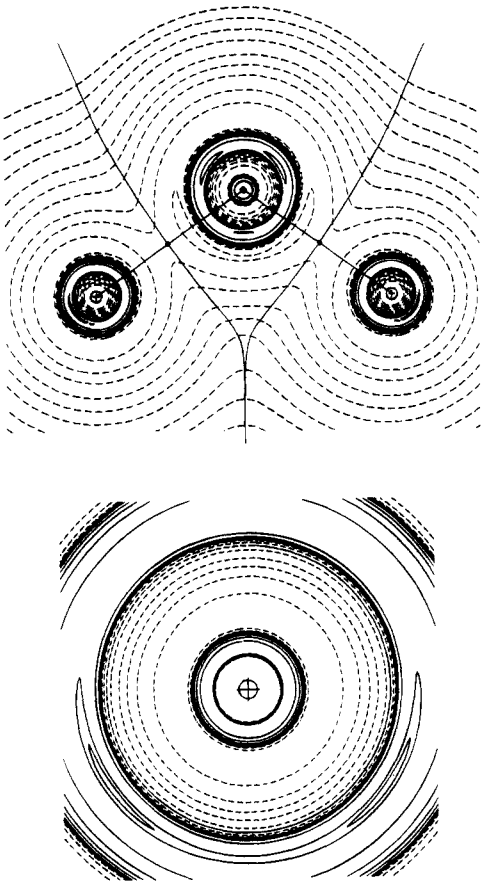

Figure 2. Contour maps of $\nabla^2\varrho$ for CaF_2 for a bond angle of 109.5°. The upper plot is for the plane of the nuclei and shows the ligand-opposed charge concentrations in the calcium core. The lower plot is an expanded display for the plane through the calcium core perpendicular to the plane of the molecule to show the presence of the two nonbonding charge concentrations. An extra contour value of 4.1 au has been used in order to show the charge concentrations more clearly.

for the charge concentrations in the third, fourth, and fifth quantum shells of these elements, respectively. The degree of concentration of the density also decreases with principal quantum number, as indicated by the values in Table 3, the LOCCC's being close in value to that found for the corresponding shell of the free atom. In all cases the LOCCC's are of larger magnitude than the NBCCC's, as a consequence of their being more spatially contracted.

Unlike the case of Ca, the outer shell of charge concentration of the Sr and Ba atoms is fragmented; compare Figures 1 and 3. In the Ba molecules only four separated CCC's survive, while in the case of Sr, the two LOCCC's and the two NBCCC's are linked by charge concentrations associated with (3,−1) critical points which lie in the plane of the nuclei between the maxim.

Table 3 also lists the angle made by the positions of the critical points defining the maxima for each pair of CCC's and the metal nucleus, ∠cc−M−cc. While a LOCCC is intersected by the continuation of the metal−ligand axis as indicated in Figures 1−3, the critical point defining the position of the maximum value in general lies off this axis and the associated angle ∠cc−M−cc is always smaller than the bond angle. For the fluorides and hydrides of strontium and barium, the angle formed by the LOCCC's is approximately tetrahedral, while for the equilibrium geometries of the calcium compounds it is greater than tetrahedral but approaches the tetrahedral value as the bond angle is decreased. The corresponding angle formed by the NBCCC's exceeds the tetrahedral value for the barium

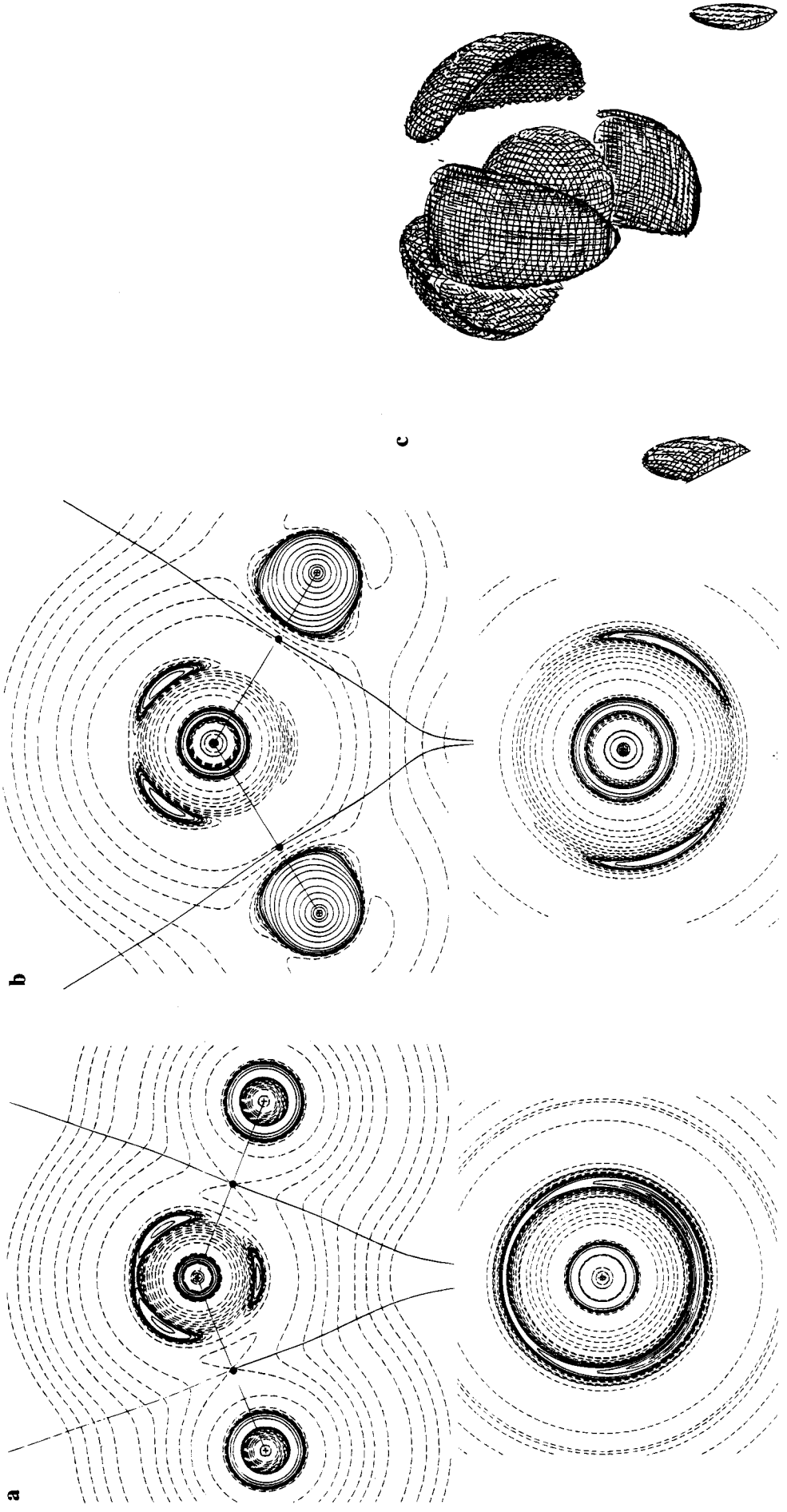

Figure 3. Contour plots of $\nabla^2\rho$ for (a) SrF_2 and (b) BaH_2. The upper plot is for the plane containing the nuclei and showing the LOCCC's, and the lower plot is for a plane obtained by a 90° rotation about the C_2 axis and showing the NBCCC's (values in Table 3). Note that the outer shell of charge concentration of the core is fragmented in these molecules. What appears to be a third maximum in the outer core of Sr in the plane of the nuclei is actually a (3,−1) critical point in $-\nabla^2\rho$, connecting the two NBCCC's, whose positive curvature is perpendicular to the plane. The spike-like maximum for the innermost core of the metal atom and the ring of charge concentration for the second shell are not separated in the upper figures. In the lower figures, the boundary contours defining the second and third concentration shells in Sr and the third shell in Ba do not contain intervening contours. (c) The zero envelope of the Laplacian distribution for the Ba core in BaH_2 showing the four charge concentrations in the outer shell of the core and the spherical inner core. The two charge concentrations in the lower part of the diagram are portions of the charge concentrations enveloping the protons.

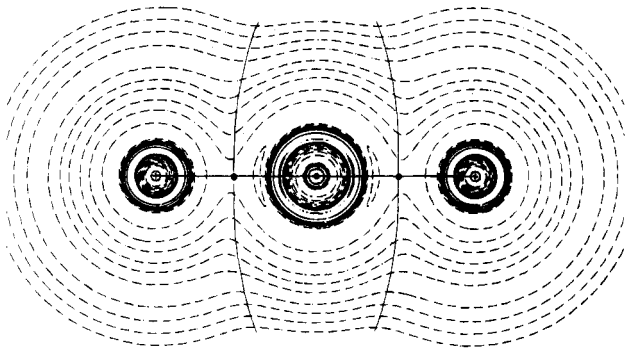

Figure 4. Contour map of $\nabla^2\varrho$ in the plane of the nuclei for linear CaF_2. Two maxima of charge concentration in the calcium core can be seen, one along each Ca−F bond, as well as one above and another below the calcium nucleus where the torus of nonbonded charge concentration intersects this plane. The torus and the axial maxima are difficult to separate in the diagram because they have similar values, −3.96 and −4.04 au, respectively, with very shallow intervening minima. The localization of electronic charge is much less pronounced in the higher energy linear geometry.

compounds but is more similar to the LOCCC values in the case of strontium. Note that the angle formed by the NBCCC's is greater for the Ba compounds than for the corresponding Sr compounds, indicating that this angle increases as the bond angle decreases and the ligands approach the NBCCC's. Note as well the remarkable similarity in the values of the CC's and in the angles they form with the Ca nucleus for the dihydride and dimethyl molecules. The hydride and methyl ligands, each with a charge of ~−0.83 e and each with its boundary a distance 2.21 au from the Ca nucleus, exert similar fields on the Ca core.

Reference to Figure 4 shows that, in the linear CaF_2 molecule, the outer core of the Ca atom exhibits a torus of charge concentration encircling the axis and a localized charge concentration opposite each of the fluorines. On bending of the molecule, it is this torus of charge concentration that first breaks to become an arc in the plane perpendicular to the molecular plane, Figure 1, and then separates into two localized charge concentrations, Figure 2. The two axial charge concentrations retain their ligand-opposed positions as the molecule bends, each following the motion of the opposing fluorine atom, Figure 2. This dynamic view of the behavior of these CCC's justifies their labelling as ligand-opposed.

The approximately tetrahedral arrangement of the charge concentrations in the outer shell of the cores of the metal atoms in these compounds corresponds closely to the qualitative model proposed earlier.[7,8] The repulsive interaction of the F^- ions with the electrons in the outer shell of the core coupled with the Fermi (spin) correlation causes their partial condensation into four localized pairs.[9] The resulting four CCC's, two LOCCC's, and two NBCCC's are arranged in an approximately tetrahedral manner, as anticipated on the basis of the VSEPR model. This tetrahedral arrangement of four charge concentrations in the outer shell of the core of calcium is reminiscent of the tetrahedral arrangement of four charge concentrations in the valence shell of the oxygen atom in a molecule such as H_2O, corresponding to the presence of two bonded and two nonbonded pairs. The tetrahedral arrangement in this case arises from the *attraction* of the two protons for the valence density, acting in conjunction with the Fermi (spin) correlation. In contrast, in the molecules considered here, it is the *repulsion* by the two negatively charged ligands of the electrons in the outer shell of the core of Ca^{2+} coupled with the spin correlation that produces two LOCCC's and two NBCCC's, with an overall tetrahedral arrangement. Thus core charge concentrations behave just like valence shell charge concentrations within the VSEPR model in that they tend to keep as far apart as possible, but they differ in their behavior by being spatially opposed to a ligand, rather than appearing as a bonding concentration. The bent geometries of the fluorides and hydrides of Ca, Sr, and Ba and of $Ca(CH_3)_2$ may be visualized as resulting from the minimization of the repulsion of the negatively charged ligands by the tetrahedral arrangement of the CC's of the core, with the ligands occupying positions opposite two faces of the tetrahedron, that is, opposite ring critical points. These are the points, 4 in number, where $-\nabla^2\varrho$ exhibits its minimum values in the outer shell of the core and where the electronic charge is least concentrated. In the Sr and Ba molecules, where the outer shell of charge concentration of the core is fragmented, the Laplacian exhibits positive values at the ring critical points (Figure 3). Thus the CC's on the ligands act as bases and pair up with "holes" on the metal cores, in the manner of a Lewis acid−base reaction.[18] Minimization of the repulsion between the ligands and the CCC's is balanced against the repulsion between the ligands themselves, resulting in bond angles that decrease with increasing size and polarizability of the core. In the higher energy linear geometry, the ligands are in each case directly opposed to a CCC. Further support of this interpretation appears in the form of the VSCC of the fluorines, as discussed below.

Similar core charge concentrations have been observed previously in the VCl_3 and $VOCl_3$ molecules.[26] For example, the vanadium core in the planar VCl_3 molecule exhibits two NBCCC's in addition to three LOCCC's. The five charge concentrations have an overall trigonal bipyramidal geometry with the LOCCC's in the equatorial positions and the NBCCC's in the axial positions. This geometry is similarly rationalized on the basis of a maximal avoidance of the core CCC's with the negatively charged ligands, the CCC's themselves being arranged in the manner anticipated on the basis of the VSEPR model. In terms of the orbital model, the outer shell of the vanadium core in VCl_3 has 10 electrons with the configuration $3s^23p^63d^2$, and these occupied orbitals can be used to construct a set of sp^3d hybrids to describe the trigonal bipyramidal geometry of the core distortion. Similarly, the distortions of a Ca, Sr, or Ba core can be described in terms of a set of four tetrahedral sd^3 hybrids constructed from the s and d orbitals, this description providing a rationalization of the use of d type polarizing functions in the *ab initio* calculations. However, it is not always possible to construct a set of hybrid orbitals within the valence bond model that accounts for the observed pattern of CCC's, the patterns observed in $CrOF_4$ and $MoOF_4$ being two cases in point.[27]

Linear MgF_2. The BeF_2 and MgF_2 molecules have been observed experimentally and predicted by *ab initio* calculations to be linear, and it is of interest to examine the Laplacian distribution of the MgF_2 molecule and contrast its properties with those of the bent difluorides. The equilibrium geometry of the magnesium fluoride molecule, calculated at the MP2-(FULL)/6-311G* level, was found to be linear. The Laplacian of the electron density (Figure 5) shows that the core is distorted but in a different manner from that found for the Ca core. There is a charge concentration maximum between the Mg nucleus and each fluoride ion but no torus of charge concentration in the plane perpendicular to the plane of the molecule. These two charge concentrations are the only ones present in the core of Mg even when the molecule is bent, whereas there are four

(26) MacDougall, P. J.; Hall, M. B.; Bader, R. F. W.; Cheeseman, J. R. *Can. J. Chem.* **1898**, *67*, 1842.
(27) Gillespie, R. J.; Bytheway, I.; de Witte, R. S.; Bader, R. F. W. *Inorg. Chem.*, to be submitted for publication.

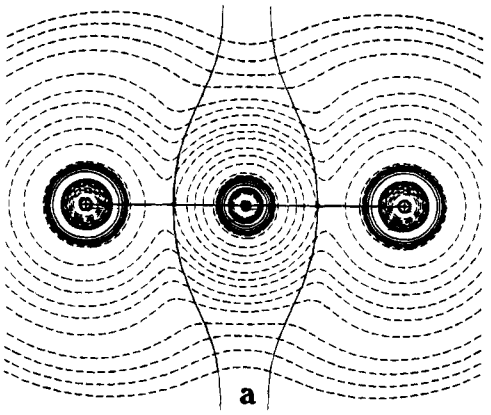

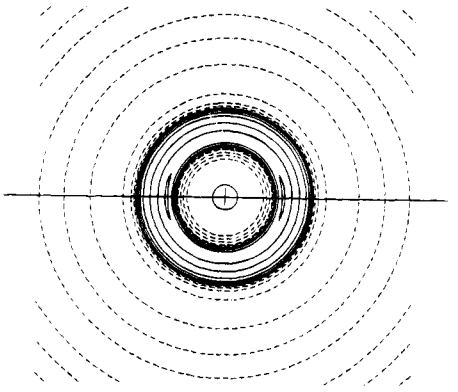

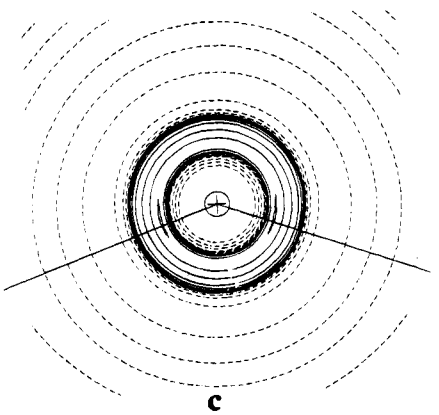

Figure 5. (a) Contour map of $\nabla^2\varrho$ in the plane of the nuclei for the MgF_2 molecule for a bond angle of 180°. (b) An enlarged view of the Mg core for the linear case. (c) An enlarged view of the Mg core for a bond angle of 140°. An extra contour of value 57 au has been used to show the charge concentrations, which are of small spatial extent, more clearly. Note that in this case the charge concentrations follow the motion of the ligands on bending in the manner of bonded charge concentrations.

charge concentrations in the core of Ca in the bent molecule. Moreover, the two CCC's of Mg follow the fluoride ions when the molecule is bent, behaving just like the bonding CC's in a main group fluoride such as SF_4,[25] whereas the two CCC's on the molecular axis in the linear CaF_2 molecule behave as LOCCC's and remain on the opposite side of the core from each fluoride ion as the molecule bends.

The important observation within the extended VESPR model in accounting for the different geometries of the magnesium and the heavier metal difluorides is not the relative magnitudes of the CCC's, which are necessarily greater for the second quantum shell of Mg than are those for the third and higher shells of Ca, Sr, and Ba (Table 3), but rather the difference in

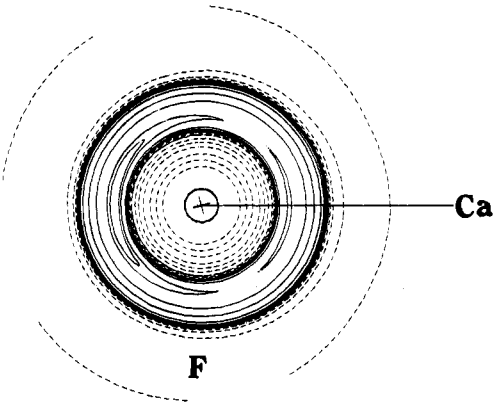

Figure 6. Plot of $\nabla^2\varrho$ for a fluorine in the minimum-energy CaF_2 molecule. The two charge concentrations along and behind the Ca–F bond are shown. Two extra contours were used in this plot in order to show these maxima, features which do not appear in the contour maps for $\nabla^2\varrho$.

the *form* of the distortions of the cores in the two sets of molecules induced by the negatively charged ligands. In MgF_2, only two CCC's are formed, and they behave like bonding charge concentrations, the linear geometry maximizing the separations between the two CCC's and between the two fluorine ligands. The presence of four CC's in the cores of the heavier alkaline earth elements, tetrahedrally arranged for maximum avoidance as anticipated on the basis of the VESPR model, results in a bent geometry, the ligands avoiding the CCC's by occupying two faces of the tetrahedron.

These differing behaviors of the CCC's in Mg and the heavier metals are reflected in the Laplacian distributions of the ligands as well. A plot of $\nabla^2\varrho$ for a fluorine atom in CaF_2 (Figure 6) shows the presence of local charge concentrations in its valence shell on both its bonding and nonbonding sides with respect to the calcium atom. The fluorine atoms in the difluorides of strontium and barium exhibit the same pattern of VSCC's. A bonding charge concentration on the fluorine atom is unusual and has previously been found only in hydrogen fluoride.[9] Thus in magnesium difluoride, these bonding and nonbonding VSCC's on fluorine are absent and replaced by (3,−1) critical points, there being instead a torus of nonbonded charge concentration about the internuclear axis encircling the F nucleus. This is the behavior usually encountered in fluorine-containing molecules of main group elements, SF_4 for example, where the VSCC's belonging to the fluorines are not along the bonds but in a plane roughly perpendicular to the S–F bond.[25] Thus in cases where a bonding charge concentration is found on the central ion, no such concentration is present on the fluorine atom—which is the case for MgF_2. However, when no bonding charge concentration is present on the central ion, then a bonding charge concentration is supplied by the fluorine—the case for the heavier metal difluorides. This behavior can be incorporated into the model in terms of an avoidance of charge concentrations on the central ion by those on the ligands. In MgF_2 the bonding charge concentrations are on the cation and avoided by the VSCC's on the ligands, whereas in CaF_2, SrF_2, and BaF_2 the bonding charge concentrations are supplied by the ligands and they are avoided by both the LOCCC's and the NBCCC's on the cation, the ligands occupying the faces of the tetrahedron of charge concentrations found on the core.

Comparison with the Polarized Ion Model. The observation that bent structures are favored by large cations and small anions is understandable in terms of Guido and Gigli's results.[17] These authors find that the main force causing an alkaline earth

Table 4. Atomic Moments[a] as a Function of Bond Angle in MgF_2 and CaF_2

	monopole		dipole[b]		quadrupole[c]	
atom	∠FMF = 180°	∠FMF = 140°	∠FMF = 180°	∠FMF = 140°	∠FMF = 180°	∠FMF = 140°
Mg	+1.760	+1.765	0.000	0.025	0.578	0.469
F	−0.880	−0.883	0.327	0.341	0.808	0.883
Ca	+1.799	+1.823	0.000	0.168	0.505	0.443
F	−0.900	−0.912	0.120	0.128	1.046	1.059

[a] In atomic units. [b] Negative end of dipole on M is directed along the symmetry axis, away from fluorines. Negative end of dipole on F is directed along the F−M axis toward the metal atom. [c] This is the single positive component of the traceless quadrupole tensor. In the linear molecule it is coincident with the molecular axis.

dihalide molecule to bend is the interaction of the negative charge on the ligands with the dipole they induce on the cation, a dipole which is necessarily zero in the linear molecule but becomes progressively larger on bending. This force predominates only when the cation is large and substantially polarized by small anions. One anticipates a substantial difference in the polarizabilities of the Mg core and cores of the heavier alkaline earth metals. The polarization of the Mg core, a closed shell, requires the mixing in of the 3s and 3p orbitals of the next quantum shell whereas the outer shell of the Ca, Sr, or Ba core is incomplete and more easily polarized, as it requires only the mixing in of d orbitals from the same quantum shell.

The atomic moments can be determined using the theory of atoms in molecules,[18] and a comparison of the dipole moments induced in the electron distributions of the Ca and Mg atoms upon bending their difluorides quantifies the assumptions of the polarized ion model, Table 4. The positive charge on Ca is larger than that on Mg, and the charge on Ca increases significantly with bending. Bending does indeed induce a considerably larger polarization of the density of the Ca core than of the Mg core, with the electron density of the cation being pushed away from the ligands along the C_2 symmetry axis. The moment for Ca attains a magnitude of 0.168 au (0.427 D) at the experimental bond angle of 140° while the magnitude of this same moment for Mg is only 0.025 au for the same degree of bending. The dipolar polarization of a fluorine ligand is directed along the M−F bond and is larger for MgF_2 than for CaF_2, 0.327 compared to 0.120 au. However, these values change little on bending, and hence the interaction of the ligand dipole with the charge on the cation does not contribute to the *bending* force. The atomic quadrupole moments, which are not included in the polarized ion model, are similar for metal and ligand in both molecules and, like the dipoles on the fluorines, are less sensitive to the degree of bending than are the induced dipoles on the metals.

The dipoles induced in the cores of the Sr and Ba cores are significantly greater than that for Ca, reflecting their greater polarizability and ease of bending. Thus the atomic moments of Sr in its difluoride and dihydride are 0.199 and 0.288 au, respectively, while the corresponding moments for Ba are 0.505 and 0.699 au, the latter corresponding to an induced dipolar polarization equal to 1.78 D. The metal-directed dipoles induced on the ligands are smaller than those in the Mg and Ca molecules, equaling 0.039 and 0.089 au for H in SrH_2 and BaH_2, respectively, and 0.059 and 0.041 au for F in the corresponding fluorides. Thus the calculated atomic moments substantiate the findings of the polarized ion model that the principal force leading to bending is the interaction of the charge on the ligands with the bending-induced dipole of the cation, an interaction that is overriding for polarizable cations and compact anions.

The distortion of the core density revealed by the topology of the Laplacian of the electron density is different from and complementary to the polarization of the core described by its induced dipole and quadrupole moments. The polarized ion model attributes the differing geometries of BeF_2 and MgF_2 molecules and the heavier alkaline earth compounds to the differing extents of dipolar polarization induced in the metal ion cores, while the Laplacian demonstrates that the distortions of the cores in these two sets of molecules correspond to different localizations of the electron pair density with corresponding consequences for their respective geometries.

Conclusions

This work is part of a continuing effort to explore the physical basis of the VSEPR model through the topological analysis of the Laplacian of the electron density, a measurable property,[27-32] and to thereby improve our understanding of the geometries of molecules which appear to be exceptions to the VSEPR rules.[28-33] The present study confirms the suggestion[7,8] that the deviation of CaF_2 from the linear geometry predicted by the VSEPR model can be accounted for in terms of a tetrahedral distortion of the Ca core resulting from the partial condensation of the core electrons into pairs,[9] as revealed by the local concentrations of electronic charge in the Laplacian distribution. The present and past work[26] and work in progress[27] demonstrate that the formation of ligand-opposed charge concentrations in the outer core of elements in the fourth and succeeding rows of the periodic table appears to be a general phenomenon. The study confirms the complementary explanation provided by the polarized ion model in terms of the dominance of the interaction between the charged ligands and the induced dipole on the metal ion. It appears that the very features of a core that make possible its distortion into four or more charge concentrations are the same as those that cause it to be more easily polarized. Distortions of a metal atom core can be expected to play a role in the geometry of other molecules containing a polarizable central atom. In a following companion paper[27] we show that distortion of the metal atom core in some transition metal molecules provides a simple explanation of the difference between the shapes of these molecules and analogous main group molecules.

Acknowledgment. The authors wish to thank Dr. Y. Aray for his assistance in constructing basis sets for the metal atoms.

IC940525Q

(28) Craven, B. M.; Stewart, R. F. *Trans. Am. Crystallogr. Assoc.* **1990**, *26*, 41.
(29) Lobanov, N. N.; Tsirel'son, V. G.; Belokoneva, E. L. *Russ. J. Inorg. Chem. (Engl. Transl.)* **1988**, *33*, 1740.
(30) Stewart, R. F. In *The Application of Charge Density Research to Chemistry and Drug Design*; Jeffrey, G. A., Piniella, J. F., Eds.; NATO ASI Series 250; Plenum Press: New York, 1991; p 63.
(31) Bianchi, R.; Destro, R.; Merati, F. In *The Application of Charge Density Research to Chemistry and Drug Design*; Jeffrey, G. A., Piniella, J. F., Eds.; NATO ASI Series 250; Plenum Press: New York, 1991; p 340.
(32) Destro, R.; Bianchi, P.; Gatti, C.; Merati, F. *Chem. Phys. Lett.* **1991**, *186*, 47.
(33) Downs, J. W.; Swope, R. J. *J. Phys. Chem.* **1992**, *96*, 4834.